

A Full Newton Scheme for the Coupled Schrödinger, Poisson, and Density-gradient Equations

Seonghoon Jin, Young June Park, and Hong Shick Min

School of Electrical Engineering and Nano-Systems Institute (NSI-NCRC), Seoul National University, Seoul, Korea
E-mail : sjin@isis.snu.ac.kr, Tel : +82-2-880-7285, FAX : +82-2-882-4658

Abstract— We develop a fully coupled Newton scheme for the self-consistent solution of the Schrödinger, Poisson, and transport equations, which is found to be a powerful method in several moderate sized problems. We apply the method to a new hybrid model that solves the one-dimensional Schrödinger equation in the confinement direction and the quantum corrected transport equation in the transport direction, and study the convergence behavior of the coupled scheme. Also, we check the validity of our new model using the nonequilibrium Green's function method.

I. INTRODUCTION

To simulate various quantum phenomena occurring in the nano-scale MOSFET devices, a self-consistent solution of the Schrödinger, Poisson, and transport equations is necessary [1]–[3]. In the previous works, the self-consistent solution is usually obtained in a decoupled manner because the Schrödinger equation cannot be easily coupled with other equations. Therefore, the Schrödinger equation is usually solved with a given potential to obtain its eigenvalues and eigenvectors, and outer iterations together with the Poisson and transport equations are performed to obtain the self-consistency [1]–[3]. One of the disadvantages of the decoupled scheme is its slow convergence rate. Moreover, we observe that it sometimes fails to converge to a sufficient accuracy in the high gate bias condition.

To solve these problems, we view the Schrödinger equation as a nonlinear partial differential equation (PDE), and apply a fully coupled Newton scheme [4] to solve the Schrödinger, Poisson, and transport equations simultaneously. Although the computational burden per each iteration may slightly increase compared with the decoupled scheme, the numerical error and required number of iterations decrease significantly. Moreover, the numerical factorization of the Jacobian matrix does not have to be performed per each iteration because the Newton-Richardson (N-R) acceleration technique can be applied to the coupled scheme. Therefore, the overall efficiency as well as the accuracy of the simulation can be improved by the coupled scheme when it is applied to moderate sized problems. For example, when we simulate MOSFET devices in two-dimension, we usually obtain the subband energies and wavefunctions along the channel from the one-dimensional Schrödinger equations in the vertical direction, and calculate the transport of the two-dimensional electron gas (2DEG) confined in the inversion layer using a semi-classical model. In this case, the coupled scheme can reduce the simulation time about an order of magnitude with a much more tight error bound compared with the decoupled scheme.

As a first simple, but nontrivial application of the coupled scheme, we develop a new hybrid model that solves the Schrödinger equation in the confinement direction and the quantum corrected transport equation in the transport direction (2DEG/DG model hereafter). It is similar to the conventional density-gradient (DG) model [5]–[7], but in our model, the vertical quantum confinement is included exactly in the Schrödinger equation, and the lateral quantum effects are included approximately in terms of the effective quantum potential defined for each subband. Using the proposed model, we simulate a silicon-based double-gate MOSFET (DGFET) device and compare the efficiency of the proposed coupled scheme with the decoupled scheme. Also, we assess the accuracy of the 2DEG/DG model using a more rigorous quantum transport model based on the nonequilibrium Green's function (NEGF) method [1], [2]. All of these models are implemented in our in-house device simulator NANOCAD [7].

II. BASIC MODELS

In the mode-space approach [2], the two-dimensional Schrödinger equation is divided into the confinement (y -coordinate) and transport (x -coordinate) directions, and the Schrödinger equation in the confinement direction with a normalization condition can be written as

$$\left[\mathcal{F}_{\psi_i^k} \quad \mathcal{F}_{E_i^k} \right]^T = 0, \quad (1)$$

where

$$\begin{aligned} \mathcal{F}_{\psi_i^k} &\equiv \left[\frac{\partial}{\partial y} \frac{\hbar^2}{2m_y^k} \frac{\partial}{\partial y} - \bar{V}(x, y) + E_i^k(x) \right] \psi_i^k(x, y) \\ \mathcal{F}_{E_i^k} &\equiv \int_{-\infty}^{\infty} [\psi_i^k(x, y)]^2 dy - 1 \end{aligned} \quad (2)$$

In the above equations, k (1, 2, 3) and i (1, 2, ..., N_{sub}) denote the valley and subband indexes, $\bar{V} \equiv V + \Delta V$ is the sum of the electrostatic potential energy (V) and the Si-SiO₂ band offset (ΔV), and ψ_i^k and E_i^k are the wavefunction and the energy of the subband (k, i), respectively. The closed boundary condition is imposed on both sides of the y -domain. Instead of finding ψ_i^k and E_i^k by the conventional eigensystem solution routines, we can directly obtain them by the Newton method with appropriate initial guesses for ψ_i^k and E_i^k , which is the basic idea of this work. In the self-consistent calculations, the equations for the different subbands are coupled to one another through the Poisson equation.

Whereas the electron density in each subband is obtained from the energy dependent local density of states (LDOS)

and their occupations in the NEGF model, the LDOS is not available in the DG model. Instead, it is assumed that the transport occurs near equilibrium and the scattering process is dominant, and the subband density (N_i^k) is expressed in terms of the quasi-Fermi energy (E_{Fi}^k) and the quantum potential (V_{Qi}^k) by

$$\begin{cases} N_i^k(x) &= n_0^k F_0 \left[\frac{E_{Fi}^k(x) - E_i^k(x) - V_{Qi}^k(x)}{k_B T} \right] \\ V_{Qi}^k(x) &= -\frac{1}{\sqrt{N_i^k(x)}} \frac{\partial}{\partial x} \left[\frac{\hbar^2}{2m_x^k r} \frac{\partial \sqrt{N_i^k(x)}}{\partial x} \right], \end{cases} \quad (3)$$

where $n_0^k \equiv g_k \sqrt{m_x^k m_z^k} k_B T / (\pi \hbar^2)$ is the density of states for the subbands in the k -th valley, and $F_0(x) \equiv \ln[1 + \exp(x)]$ is the Fermi-Dirac integral of order zero. Note that the quantum potential is separately defined for each subband (k, i) to include the effects of the anisotropic band structure. The theoretical value of the dimensionless coefficient r is 3 according to the microscopic derivation of the quantum potential from the Wigner distribution function in the nondegenerate limit [6]. The two equations in (3) can be condensed into one as

$$\mathcal{F}_{N_i^k} \equiv \left[\frac{b^k \partial^2}{\partial x^2} + \frac{E_{Fi}^k - E_i^k}{k_B T} - F_0^{-1} \left(\frac{N_i^k}{n_0^k} \right) \right] \sqrt{N_i^k} = 0, \quad (4)$$

where $b^k \equiv \hbar^2 / (2rm_x^k k_B T)$. The quasi-Fermi energy of each subband is determined by the semi-classical transport equation as

$$\mathcal{F}_{E_{Fi}^k} \equiv \frac{\partial}{\partial x} \left(\mu_i^k N_i^k \frac{\partial E_{Fi}^k}{\partial x} \right) + \sum_{k', i'} \left(P_{ki}^{k' i'} - P_{k' i'}^{ki} \right) = 0, \quad (5)$$

where μ_i^k is the mobility of the subband (k, i), and $P_{ki}^{k' i'}$ is the local transition rate from the subband (k', i') to (k, i). Since the focus of this paper is more on the numerical aspects of the coupled scheme and the general properties of the 2DEG/DG model than on the calibration of the model, we use a simple mobility model that depends on the impurity concentration and lateral electric field, and we neglect the local transitions. More accurate mobility and local transition models, however, can be applied to our model.

Finally, the Poisson equation can be written as

$$\mathcal{F}_V \equiv \nabla \cdot [\epsilon \nabla V(x, y)] - q^2 [p - n + N_D^+ - N_A^-] = 0, \quad (6)$$

where

$$n(x, y) = \sum_{k, i} N_i^k(x) [\psi_i^k(x, y)]^2. \quad (7)$$

The coupled equations are solved by the fully coupled Newton scheme to obtain the unknown variables V , ψ_i^k , E_i^k , $\sqrt{N_i^k}$, and E_{Fi}^k as

$$\left[\frac{\partial \mathcal{F}(\mathbf{x})}{\partial \mathbf{x}} \right] \Delta \mathbf{x} = -\mathcal{F}(\mathbf{x}), \quad \mathbf{x} \rightarrow \mathbf{x} + \Delta \mathbf{x} \quad (8)$$

where

$$\begin{cases} \mathcal{F} &= [\mathcal{F}_V \quad \mathcal{F}_{\psi_i^k} \quad \mathcal{F}_{E_i^k} \quad \mathcal{F}_{N_i^k} \quad \mathcal{F}_{E_{Fi}^k}]^T \\ \mathbf{x} &= [V \quad \psi_i^k \quad E_i^k \quad \sqrt{N_i^k} \quad E_{Fi}^k]^T \end{cases}. \quad (9)$$

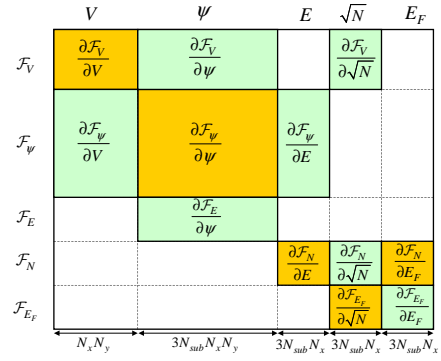


Fig. 1. Schematic of the Jacobian matrix. The total number of unknowns is $((1 + 3N_{\text{sub}})N_x N_y + 9N_{\text{sub}} N_x)$. Note that each block matrix is very sparse.

If we use a tensor grid of $N_x \times N_y$ nodes to discretize the equations, the sizes of the unknown variables, V , ψ_i^k , E_i^k , $\sqrt{N_i^k}$, and E_{Fi}^k , become $N_x N_y$, $3N_{\text{sub}} N_x N_y$, $3N_{\text{sub}} N_x$, $3N_{\text{sub}} N_x$, and $3N_{\text{sub}} N_x$, respectively. Therefore, the total number of unknowns becomes $((1 + 3N_{\text{sub}})N_x N_y + 9N_{\text{sub}} N_x)$. Fig. 1 shows the schematic of the Jacobian matrix. We use a direct sparse matrix solver and exploit the N-R acceleration technique in the Newton iteration. We use the solution of the previous bias step as an initial guess, and we use the decoupled scheme to obtain the solution of the first bias step. The voltage difference between the successive steps is chosen to be 0.05 V, which gives good convergence behavior.

We mention that the coupled scheme may lose its advantage when it is applied to large sized problems such as the NEGF model. Actually, we have implemented the coupled scheme for the ballistic NEGF model, and found that the required iteration number and numerical error indeed decreases similarly to the case of the 2DEG/DG model. But, the simulation time per each iteration becomes too long. Therefore, the coupled scheme is not always better than the decoupled scheme, but there are many applications that the coupled scheme works better.

III. SIMULATION RESULTS AND DISCUSSION

We simulate an ultra thin body DGFET device as shown in Fig. 2. We first show the typical convergence behavior of the coupled and the decoupled schemes in Fig. 3. The decoupled scheme uses a variant of the Gummel scheme [2], [3]. As expected, the coupled scheme gives rapid convergence compared with the decoupled scheme in every bias condition. Moreover, it requires much less simulation time (it takes about 80 sec in PC to obtain the I_D - V_G curve shown in Fig. 8 consists of 16 bias points), which is due to the reduced number of iterations as well as the N-R acceleration.

Since the vertical quantum confinement effects are relatively well known and accurately included in our model, we directly move on to the lateral quantum effects. To verify the validity of the lateral quantum correction in the 2DEG/DG model, we show several important physical quantities along the channel direction when $V_G = -0.4$ V. The bias point is chosen

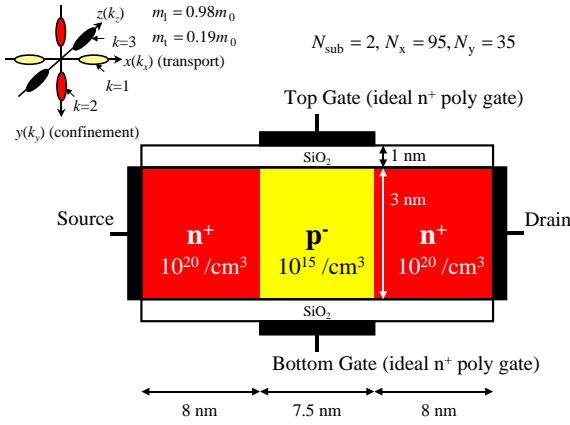


Fig. 2. Schematic of the thin body DG-FET structure. The device and crystal coordinates are aligned. The same bias is applied to the top and bottom gates.

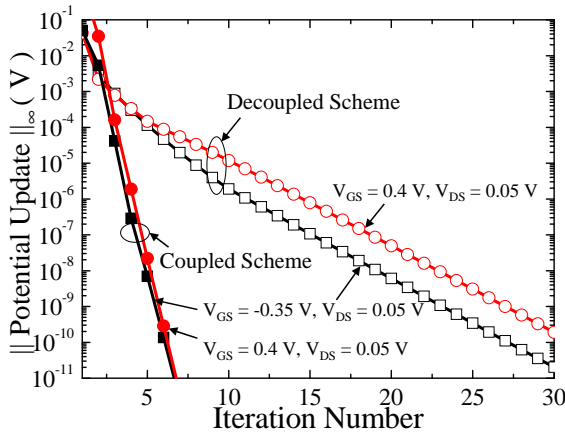


Fig. 3. Comparison of the convergence behavior between the coupled scheme and the decoupled scheme. The previous bias steps (V_G increases by 0.05 V for each bias step) are used as the initial guesses. In the coupled scheme, actual numerical factorizations occur only at the first two or three iterations.

because the lateral quantum effects are more significant in the off state. Fig. 4 shows the electron density along the x -direction predicted by the 2DEG/DG model with several different values of r and the NEGF model. The lateral quantum correction becomes weaker as r increases, and when $r = \infty$, the lateral quantum correction vanishes. The electron density predicted by the 2DEG/DG model with $r = 3$ (theoretical value) is very close to the value predicted by the NEGF model, which suggests that the quantum potential equation reasonably takes into account the lateral quantum effects. To see the effects of the lateral quantum correction on the relative occupations of electrons between subbands, we show the subband densities along the channel in Fig. 5. Subband densities predicted by the 2DEG/DG model agree well with the NEGF model. Note that the difference between N_1^1 and N_1^3 is due to the difference in the lateral quantum correction, which depends on the lateral effective mass as shown in (3). Fig. 6 shows the subband energy levels and quantum potentials along the channel. Since the m_x of the valley 1 corresponds

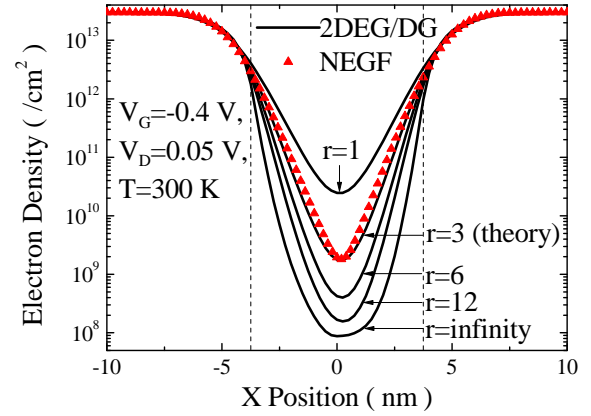


Fig. 4. Electron density along the channel ($\sum_{k,i} N_i^k(x)$) predicted by the 2DEG/DG model with different values of r (line) and the NEGF model (symbol). The lateral quantum correction becomes weaker as r increases. When $r = \infty$, the lateral quantum correction vanishes.

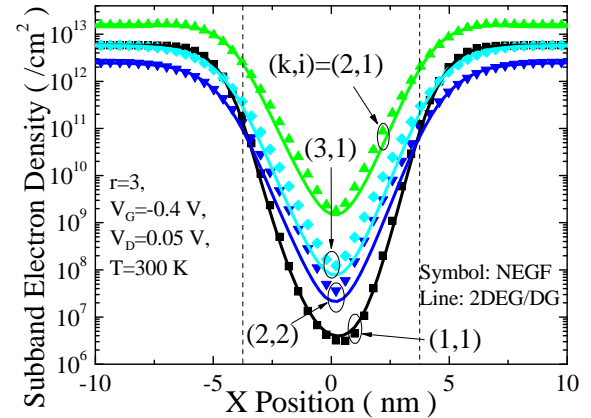


Fig. 5. Subband electron densities along the channel predicted by the 2DEG/DG (line) and NEGF (symbol) models.

to the longitudinal effective mass ($0.98m_0$), whereas those of the valley 2 and 3 are equal to the transverse effective mass ($0.19m_0$), the magnitude of the quantum potential for the valley 1 is smaller than those of 2 and 3. Also, we can see that E_1^1 and E_1^3 are equal, which means that the quantum effects along the vertical direction are same because the effective masses in the vertical direction are same in these valleys.

Fig. 7 shows the bias dependence of the minimum subband energy level predicted by the 2DEG/DG model and the NEGF model. We first increase the gate bias from -0.4 V to 0.2 V with the drain bias fixed to 0.05 V, and then we increase the drain bias from 0.05 V to 0.35 V. The agreements between the 2DEG/DG model and the NEGF model are good for the low drain bias conditions. As the drain voltage increases, however, the two models predict slightly different behaviors. In the NEGF model, the potential drop occurs only in the channel region because the scattering is neglected, whereas the 2DEG/DG model predicts that there exist slight potential drops in the source and drain regions as well because of the

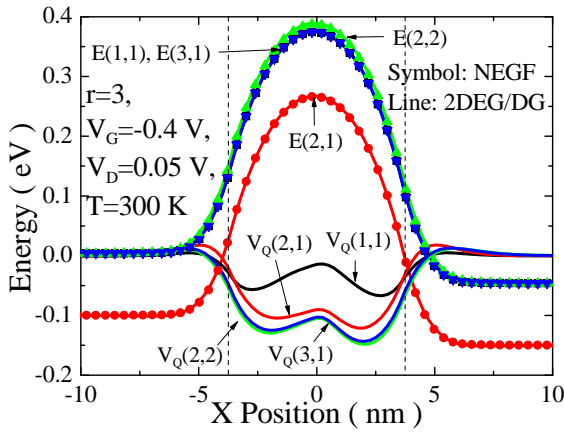


Fig. 6. Subband energy levels and quantum potentials along the channel predicted by the 2DEG/DG model (line). Subband energy levels predicted by the NEGF model are also shown (symbol).

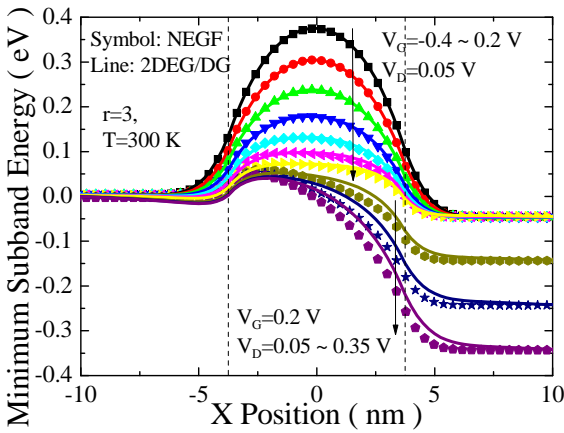


Fig. 7. Bias dependence of the minimum subband energy level predicted by the 2DEG/DG model (line) and the NEGF model (symbol). The gate bias is first increased from -0.4 V to 0.2 V with the drain bias fixed to 0.05 V, and then the drain bias is increased from 0.05 V to 0.35 V.

finite resistances in these regions.

Fig. 8 shows the I_D - V_G characteristics predicted by the 2DEG/DG model with different values of r , where we also plot those predicted by the NEGF model in the ballistic limit. The 2DEG/DG model with $r = 3$ predicts larger subthreshold leakage current and smaller on current compared with the NEGF model, which shows the limitation of our transport model that is based on the drift-diffusion (DD) equation. In the DD equation, we assume that the carrier scattering is large enough in order to define the local quasi-Fermi level, whereas we neglect the carrier scattering entirely in the ballistic NEGF model, and the actual carrier transport occurs between these two limits. For the DGFET device under consideration, we believe that its operation condition is close to the ballistic limit because the channel length is only 7.5 nm that the electrons injected from the source do not experience enough scattering before they exit the channel. Therefore, the transport equation of our model should be revised to predict the correct I-V characteristics of the nano-scale MOSFET devices.

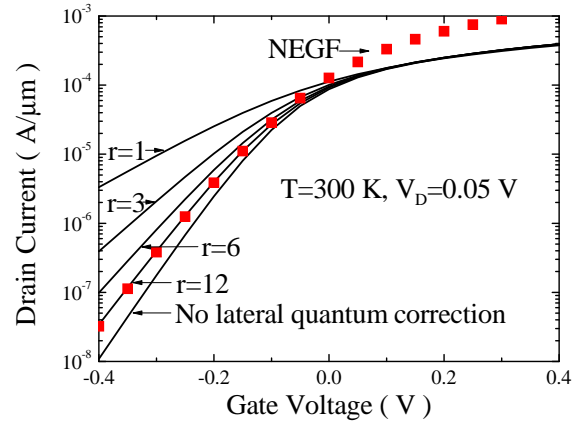


Fig. 8. I_D - V_G characteristics predicted by the 2DEG/DG model with different values of r (line) and the NEGF model (symbol).

IV. CONCLUSION

In this paper, we explained a fully coupled Newton scheme for the self-consistent solution of the Schrödinger, Poisson, and transport equations. We verified that the coupled scheme can increase the convergence rate, reduce the numerical error, and improve the overall efficiency compared with the decoupled scheme if the problem size is not too large. The coupled scheme is applied to a new hybrid model called 2DEG/DG model that solves the one-dimensional Schrödinger equation in the confinement direction and the quantum corrected transport equation in the transport direction. The predicted internal properties in near equilibrium conditions are very close to those of the NEGF model. But the I-V characteristics do not agree well with the NEGF model, which suggests that we must find out the transport equation valid at the quasi-ballistic regime.

ACKNOWLEDGMENT

This work was supported by the National Core Research Center program of the Korea Science and Engineering Foundation (KOSEF) through the NANO Systems Institute and Seoul National University.

REFERENCES

- [1] S. Datta, *Electronic Transport in Mesoscopic Systems*. Cambridge: Cambridge University Press, 1995.
- [2] Z. Ren, "Nanoscale MOSFETs: Physics, simulation and design," Ph.D. dissertation, Purdue Univ., West Lafayette, IN, USA, Dec. 2001.
- [3] S. E. Laux, A. Kumar, and M. V. Fischetti, "Analysis of quantum ballistic electron transport in ultrasmall silicon devices including space-charge and geometric effects," *J. Appl. Phys.*, vol. 95, no. 10, pp. 5545–5582, May 2004.
- [4] J. M. Ortega and W. C. Rheinboldt, *Iterative solution of nonlinear equations in several variables*. San Diego, CA: Academic Press, 1970.
- [5] M. G. Ancona and H. F. Tiersten, "Macroscopic physics of the silicon inversion layer," *Phys. Rev. B*, vol. 35, no. 15, p. 7959, May 1987.
- [6] M. G. Ancona and G. J. Iafrate, "Quantum correction to the equation of state of an electron gas in a semiconductor," *Phys. Rev. B*, vol. 39, no. 13, p. 9536, May 1989.
- [7] S. Jin, Y. J. Park, and H. S. Min, "A numerically efficient method for the hydrodynamic density-gradient model," in *Intl. Conference on Simulation of Semiconductor Processes and Devices*, Boston, Sept. 2003, p. 263.